Available online at www.eccomasproceedia.org
Eccomas Proceedia SMART (2023) 35-46

ECCOMAS Proceedia

X ECCOMAS Thematic Conference on Smart Structures and Materials
SMART 2023
D.A. Saravanos, A. Benjeddou, N. Chrysochoidis and T. Theodosiou (Eds)

FUNCTIONAL FATIGUE OF SMA-BASED ACTUATORS

LOPES LEAL JÚNIOR, M. L.[1,2,3*], PINO, L.[1], BARATI, M.[2,3,4] SAINT-SULPICE, L.[1], DANIEL, L.[2,3] AND ARBAB CHIRANI, S.[1]

[1,*]ENI Brest, UMR CNRS 6027, IRDL, F-29200 Brest, France. e-mail: lopes@enib.fr

[2] Université Paris-Saclay, CentraleSupélec, CNRS, Laboratoire de Génie Électrique et Électronique de Paris, 91192, Gif-sur-Yvette, France.

[3] Sorbonne Université, CNRS, Laboratoire de Génie Électrique et Électronique de Paris, 75252, Paris, France.

[4] Institut Polytechnique des Sciences Avancées, IPSA, 94200, Ivry-sur-Seine, France.

Abstract. Shape Memory Alloys (SMA) are an interesting option for high-compacity actuators. Meanwhile, the complexity of the precise actuation and, in particular, the variation of functional properties throughout their lifetime are major challenges for their use. The main objective of this work is to estimate the cyclic functional properties (transformation strain and residual strain) of a NiTi SMA actuator to establish methods for dimensioning actuators in a low-cycle fatigue context. In this study, experimental tests simulating the actuator operation over its lifespan were performed by using an ad-hoc test setup. Obtained results demonstrate the viability of energy-based methods for estimating functional fatigue properties.

Key words: SMA, Functional Fatigue, SMA-based actuators, NiTi, fatigue criterion, martensite transformation

1 INTRODUCTION

Smart materials are those which are able to convert a type of energy to another, at the material scale, through a state coupling phenomenon. These characteristics can be found in some specific classes of material such as piezoelectrics, piezomagnectics, and shape memory alloys (SMAs) [1, 2].

Being one of the few materials capable of converting mechanical external stimuli into a thermal response and able of recovering their original shape, SMA can be considered one

Peer-review under responsibility of the organizing committee of SMART 2023.
doi: 10.7712/150123.9762.444429

of the most interesting smart materials. These attributes are possible due to a diffusionless process called martensite transformation. The conjunction of those characteristics and the fact that SMAs have one of the bigger ratios of actuation energy density makes them a very suitable option for actuation purpose [3].

Therefore, SMA-based actuators are a convenient solution for several actuation applications, providing engineers with a compact and lightweight solution. Meanwhile, one of the main drawbacks and the major causes for its minor utilization in the industry is the variation of its thermomechanical behavior during a long-term operation.

The evolution in SMA behavior is mainly caused by the accumulation of dislocations (plasticity) and residual stress-induced martensite (RSIM) (due to internal stress accumulation) [4, 5, 6] that will change little by little, but substantially, the microstructure of the SMA. These changes can be noted and measured macroscopically. In literature, when the actuator performance is investigated, this instability is alternatively addressed as functional fatigue (FF).

Differently from structural (conventional) fatigue which focuses on the maximum number of duty cycles, FF aims at the evolution of the so-called functional properties that are linked to the actuator operation during its lifespan [7]. In this context, the main functional properties are the transformation strain (ε^{tr}), the residual strain (ε^{r}) and the phase transformation temperatures which together can provide the necessary information to evaluate the actuator output (displacement and force).

Despite a large number of investigations on fatigue in SMA-based actuators, the FF has not been studied as extensively. Some authors have studied the impact of different conditions during actuation such as the imposed mechanical stress [6], the heating current (when an actuator is heated by using the Joule effect) [8, 9, 10], the heat treatment [11], and other parameters. However, very few analyzed the impact of the main operating parameters together. Other studies have proposed criteria to define structural fatigue, but none, to the best of our knowledge, proposed criteria/relations that predict the FF when the most influential operating parameters such as heating time, cooling time, current level, stress level, and size are considered.

As some authors [12, 13] have introduced, the analysis of the so-called actuation energy can provide a great amount of information about the state of the SMA at the beginning and during the operation. This parameter evaluates the amount of energy consumed or dissipated during the actuation of the system (the work energy output). The purpose of the present work is to analyze the impact of the main operating parameters of an SMA-based actuator over its lifespan and to propose a criterion that will help predict the FF by using initial/design operating parameters and an "energy type" approach inspired by the aforementioned references.

2 MATERIALS AND EXPERIMENTAL PROCEDURES

2.1 Experimental conditions

In the present work, a 0.19mm diameter trained NiTi wire produced by Dynalloy® has been considered for the experimental tests to simulate the actuation of an SMA-based actuator over its lifespan. The wire shape is commonly implemented in SMA-based actuators when a greater output force for the actuator is necessary. Spring shapes are typically selected in order to privilege a bigger displacement output [14].

Thermomechanical loading experiments were performed by using an ad hoc testing machine (figure 1) in which the samples were heated by using the Joule effect, cooled by using two electric commanded fans and mechanically loaded by using a dead weight.

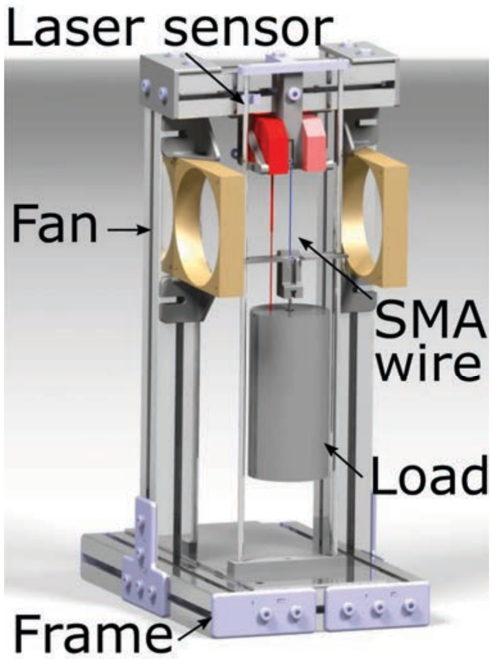

Figure 1: Ad hoc testing machine.

Different testing conditions were applied by varying the applied constant mechanical load (σ), the electrical current (i), and the heating time (HT). All the tests were conducted under forced convection regime during cooling for 2 seconds per cycle (CT). Subsequently, the experimental data were processed and the functional parameters such as, (ε^{tr}) and (ε^{r}), were extracted for each cycle until failure or up to 130k cycles when the experiments were stopped.

The loading conditions were defined in a preliminary study in which, firstly, a differential scanning calorimetry test (DSC) (figure 2) was performed in order to evaluate the phase transformation temperatures of the employed wire. Then, a wide range of values for HT, CT and σ was tested, and only the sets of parameters that allow an initial ε^{tr} bigger than 2.5% (herein considered minimum output strain level for this actuator) were chosen to be tested in a cyclic condition. Finally, the implemented loading conditions are defined in table 1.

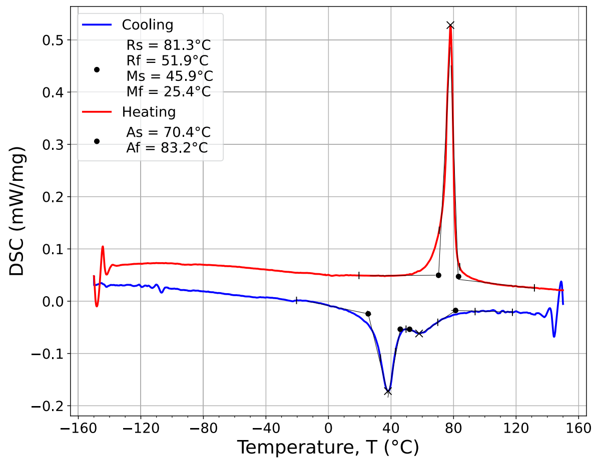

Figure 2: DSC test for the studied wire.

Table 1: Testing conditions

Test number	Stress, σ [MPa]	Heating Time, HT [s]	Cooling Time, (CT) [s]
1	100	0.55	2
2	100	0.60	2
3	230	0.50	2
4	230	0.55	2
5	230	0.60	2
6	340	0.50	2
7	340	0.55	2
8	340	0.60	2

In addition to the measured strains, another parameter ($\sigma\varepsilon_0^{tr}$) is also evaluated. This parameter is related to the maximum energy of actuation of the system and as the maximum transformation strain is obtained at the beginning of the cycling, one may consider $\varepsilon^{tr}_{max} = \varepsilon^{tr}_0$.

2.2 Functional fatigue estimation method

The design features in an SMA-based actuator are commonly the force output, the actuation frequency, the desired initial and final values for the Assisted Shape Memory Effect (ASME) and the output strain.

In this work, we will focus on the strain measurements. Then, in order to obtain the strain output of the actuator, the transformation strain (ε^{tr}), which is essentially the ASME, and the residual strain (ε^{r}) are evaluated. ε^{tr} is calculated from the difference between the maximum and minimum values of strain during actuation cycles [13, 15] and ε^{r} is calculated from the evolution of the strain at austenite phase, being directly related to the accumulation of Transformation-Induced Plasticity (TRIP) and to the Residual Stress-Induced Martensite (RSIM) in the wire and representing the unrecoverable transformation strain [4, 12].

Therefore, the combination of the two measured parameters is used to obtain the strain output of the actuator. Ideally, the strain output value must be in a range defined by the designers, that will ensure the desired displacement for the actuator during its lifespan as shown in figure 3.

Thus, the proposed FF estimation method will use only initial and the ($\sigma\varepsilon^{tr}_0$) parameters in order to help designers predict the ultimate values for ε^{tr} and ε^{r} and their evolution curves for different configurations of operating parameters. This will allow designers to estimate the FF for different actuation configurations without the need of performing several experimental tests, saving conception time and project cost.

3 RESULTS AND DISCUSSION

3.1 Evolution of the functional parameters

Given the experimental procedure, the aim of this section is to show the evolution of the functional parameters with regard to the different loading conditions. All the measured functional parameters are shown until 130k cycles or until the failure of the wire. First, for the transformation strain degradation (figure 4), one may note that the higher value for this parameter is found at the beginning of the lifespan. Then, an exponential evolution takes place until about 3-5k cycles, this stage is also called “accommodation”. Finally, an almost linear evolution occurs and continues until the failure of the actuator.

A similar degradation dynamics can be observed in the residual strain. Although, in this case, the initial amount is zero at the beginning of cycling and, then it rises exponentially until accommodation and evolves linearly to its maximum value at the end

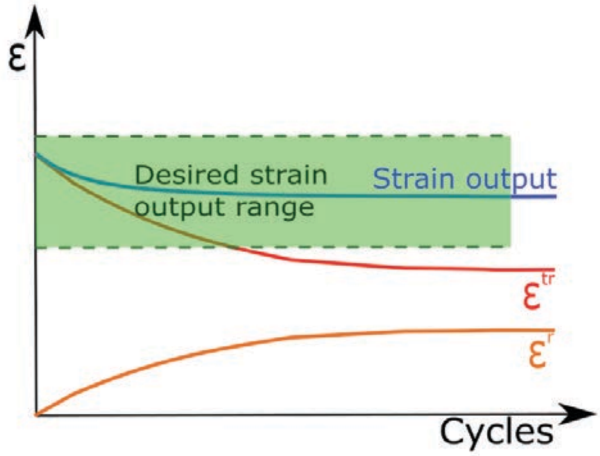

Figure 3: Desired output parameter.

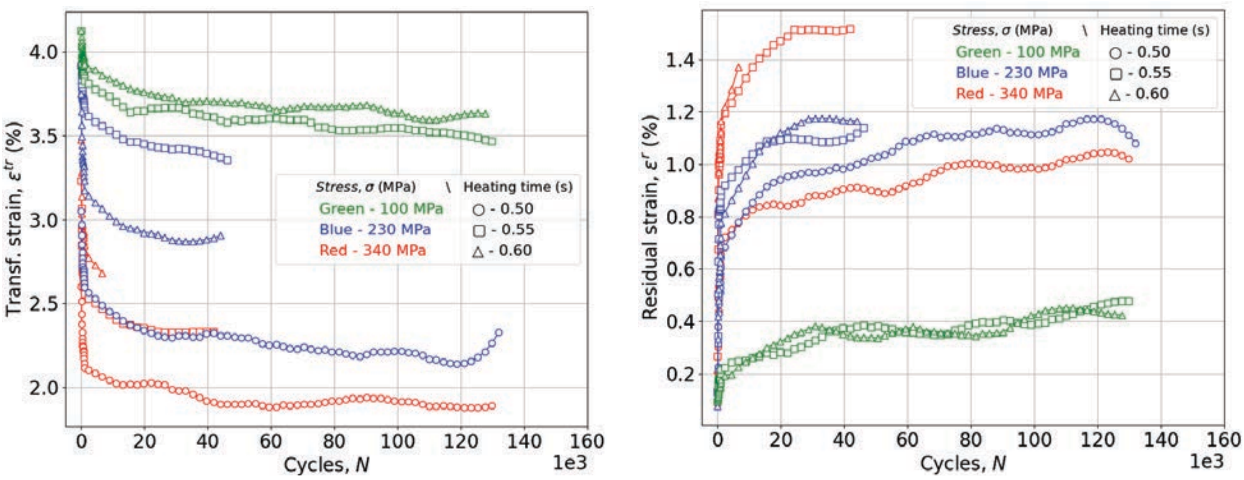

Figure 4: Transformation and residual strain evolution.

of the lifespan.

Therefore, one can note that the operating parameters (σ and HT) have a direct and strong impact on the degradation of functional parameters. With the increase of σ, the first stage of degradation seems to be more pronounced. This effect can be best observed in a logarithmic scale (figure 5), where one may note that for greater stress values, the slope of the degradation is higher than for lower stress levels. With regard to the impact of the HT, one may also note that this parameter impacts directly the amount of initial transformation strain. For the tests with the same stress level, the higher the heating time, the higher ε_0^{tr}. A similar impact of HT on the residual strain evolution is observed.

Consequently, one may infer that σ and HT impact directly the evolution of the functional parameters. Additionally, this shows that the $(\sigma\varepsilon_0^{tr})$ parameter can be a good indicator for the FF. In the next section, the viability of the proposed FF estimation method will be discussed and evaluated.

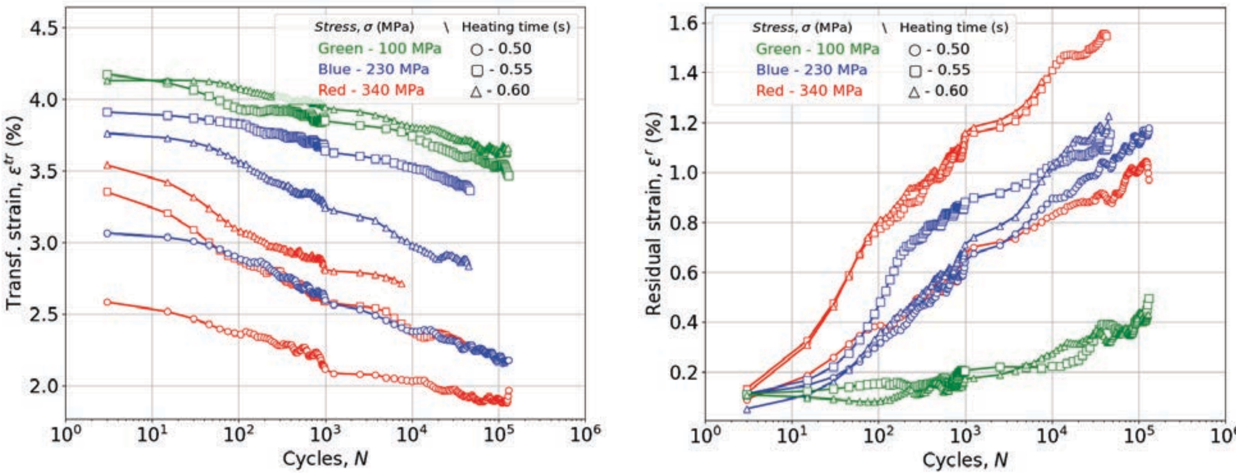

Figure 5: Transformation and residual strain evolution in logarithmic scale.

3.2 Evaluation of proposed FF estimation method

3.2.1 Ultimate values estimation

Based on the literature review and on the experimental evidence discussed previously, the goal of this section is to evaluate the proposed FF estimation method.

Firstly, an analysis of the functional parameter ε_0^{tr} for its ultimate value is performed. In figure 6, one can observe that a linear relation between the $(\sigma\varepsilon_0^{tr})$ parameter and the ultimate residual strain can be established for the majority of the testing points. This highlights that σ and ε_0^{tr} parameters have a direct influence on the residual strain. In this case, the impact of stress can be associated with the accumulation of TRIP during cycling [12, 16], where the higher the stress level, the higher the quantity of dislocations created during a cycle. Then, these additional dislocations trigger more RSIM, resulting in an increase in the residual strain. Therefore, a linear regression can be used to predict $\varepsilon_{ultimate}^{tr}$ values for different actuation configurations. The found regression coefficients and R-squared values for the proposed estimation are also presented in figure 6.

Secondly, a similar analysis is performed for ultimate transformation strain values in figure 7. However, one can note that, for this FF parameter, different linear relations can be found in each applied stress level. Therefore, as the relation is stress-dependent, one may opt for removing the stress influence from the estimation parameter $(\sigma\varepsilon_0^{tr})$.

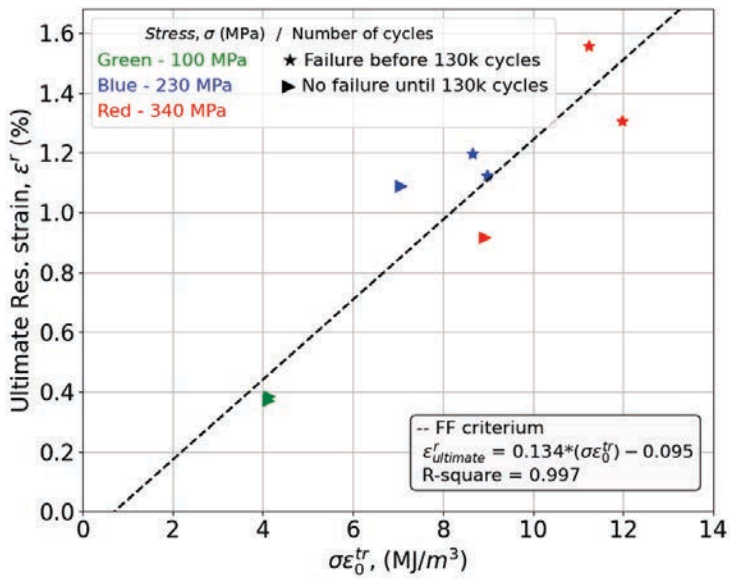

Figure 6: FF estimation for $\varepsilon^{tr}_{ultimate}$ parameter.

The stress-independence can be explained by the fact that in SMA-actuator wires, the maximum amount of transformation strain varies very little for near stress values, as the ones employed in this study. So, in this case, the major influential parameter is (ε_0^{tr}).

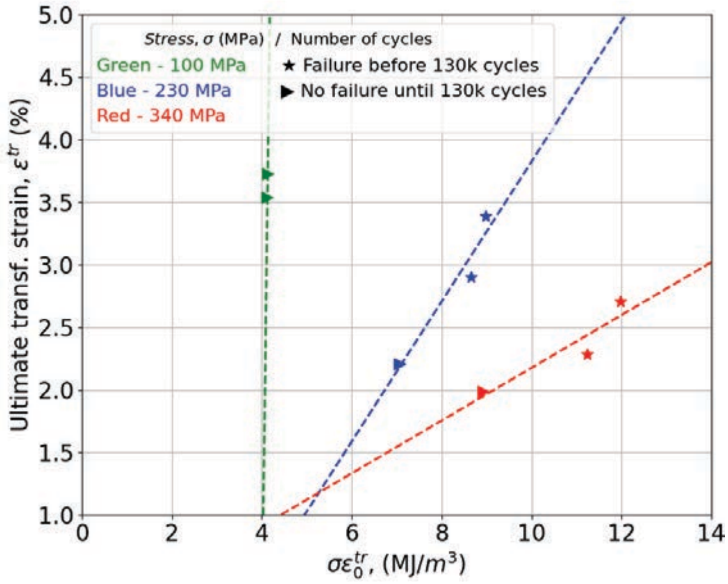

Figure 7: Linear relation between residual strain and $\sigma\varepsilon_0^{tr}$.

Finally, another linear regression is performed and the coefficients for the estimation of the ultimate transformation strain are defined and presented in figure 8. A good correspondence between the data point and the FF parameters estimations are found for both predictions.

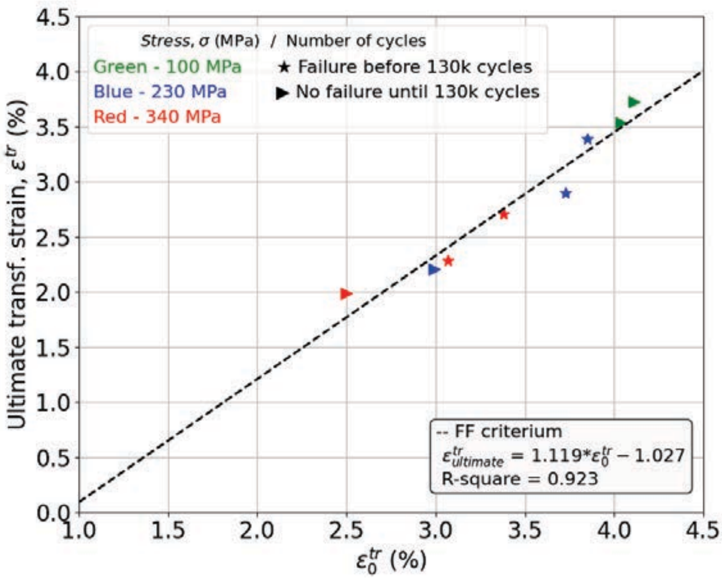

Figure 8: FF estimation for $\varepsilon^r_{ultimate}$ parameter .

3.2.2 Functional Fatigue evolution curves

In order to complete the estimation for actuators, the shape of the evolution of the aforementioned main parameters is also relevant. Based on the experimental evidences, one may note that theses parameters evolve in a logarithmic-type curve. Therefore, by using the forecast ultimate values for ε^r and ε^{tr}, the prediction of the FF evolution can be performed.

To carry out theses predictions, we opted for a description of the FF evolution until the maximum quantity of cycles (N_{max}) of 130k. Then by using the following equations:

$$\varepsilon^r = a_r * log_{10}(N), \tag{1}$$

$$\varepsilon^{tr} = a_{tr} * log_{10}(N) + b_{tr}, \tag{2}$$

where a_r, a_{tr} and b_{tr} are the evolution coefficients, evaluated from the initial parameters and from the forecast values, as follows:

$$a_r = \varepsilon^r / log_{10}(N_{max}), \tag{3}$$

$$b_{tr} = \varepsilon_0^{tr}, \tag{4}$$

$$a_{tr} = (\varepsilon_{ultimate}^{tr} - b)/log_{10}(N_{max}). \tag{5}$$

The estimations for each FF curves can be evaluated and compared with the experimental data (figure 9). By using this approach, a good correlation between the estimations and the experimental data is found, especially for those tests that reached 130k cycles. Thus, in order to increase the precision of the proposed method, a conventional fatigue criteria should be used to predict the cycles to failure and so, this value will allow to better evaluate the evolution coefficients.

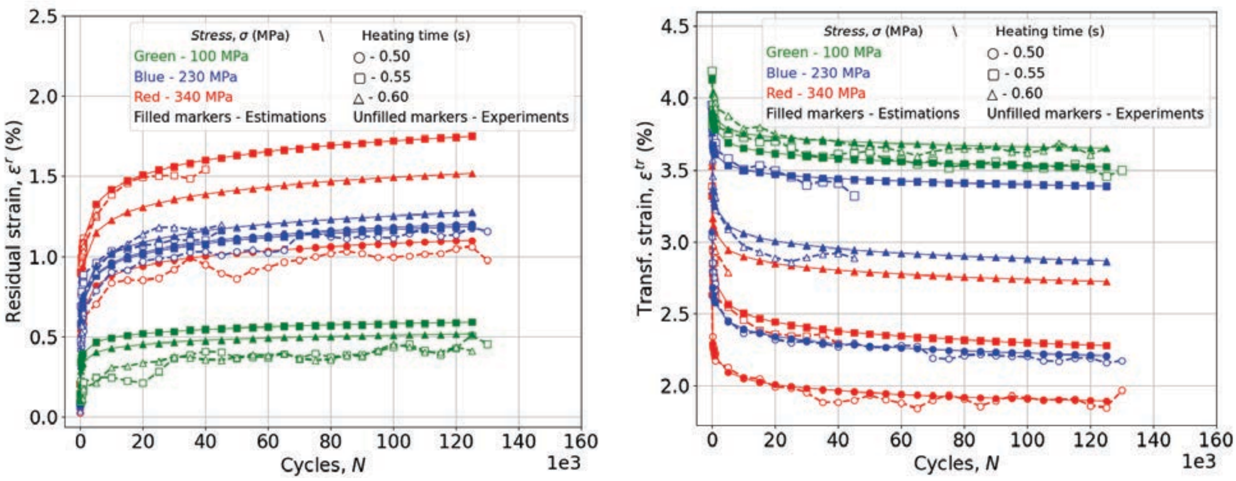

Figure 9: FF parameters evolution estimation.

4 CONCLUSIONS

In order to study the evolution of the functional parameters during actuation, fatigue tests were performed simulating a real actuation condition. The impact of the operating parameters is evaluated and it is found that the stress and the heating time are the most influential ones.

Based on the literature review and on the experimental findings, parameters related to the actuation energy ($\sigma\varepsilon_0^{tr}$) and to the initial transformation strain (ε_0^{tr}) are considered for the estimation of the ultimate values for the FF parameters. Then, the estimated values together with the design parameters are used to forecast the evolution curves of each studied FF parameter during cycling. The proposed estimations demonstrated a good correlation with the experimental data.

Finally, this approach shows an easy-to-apply solution to predict the functional properties of SMA-based actuators, helping the design and sizing procedure for this type of system. However, the stress-dependency of the two main FF parameters herein analyzed must be better investigated in order to clarify the mechanism involved in each case.

REFERENCES

[1] P. Ghosh, A. Rao, and A. R. Srinivasa, "Design of multi-state and smart-bias components using Shape Memory Alloy and Shape Memory Polymer composites," Materials & Design, vol. 44, pp. 164–171, Feb. 2013. [Online]. Available: https://www.sciencedirect.com/science/article/pii/S0261306912003731

[2] P. Kumar and D. Lagoudas, "Introduction to Shape Memory Alloys," in Shape Memory Alloys: Modeling and Engineering Applications. Boston, MA: Springer US, 2008, pp. 1–51. [Online]. Available: https://doi.org/10.1007/978-0-387-47685-8_1

[3] J. M. Jani, M. Leary, and A. Subic, Shape Memory Alloys in Automotive Applications, 2014, publication Title: Applied Mechanics and Materials. [Online]. Available: https://www.scientific.net/AMM.663.248

[4] P. Sedmák, P. Šittner, J. Pilch, and C. Curfs, "Instability of cyclic superelastic deformation of NiTi investigated by synchrotron X-ray diffraction," Acta Materialia, vol. 94, pp. 257–270, 2015. [Online]. Available: https://www.sciencedirect.com/science/article/pii/S1359645415002918

[5] R. Delville, B. Malard, J. Pilch, P. Sittner, and D. Schryvers, "Transmission electron microscopy investigation of dislocation slip during superelastic cycling of Ni–Ti wires," International Journal of Plasticity, vol. 27, no. 2, pp. 282–297, Feb. 2011. [Online]. Available: https://www.sciencedirect.com/science/article/pii/S0749641910000707

[6] Y. Gao, L. Casalena, M. Bowers, R. Noebe, M. Mills, and Y. Wang, "An origin of functional fatigue of shape memory alloys," Acta Materialia, vol. 126, pp. 389–400, Mar. 2017. [Online]. Available: https://linkinghub.elsevier.com/retrieve/pii/S1359645417300010

[7] G. Eggeler, E. Hornbogen, A. Yawny, A. Heckmann, and M. Wagner, "Structural and functional fatigue of NiTi shape memory alloys," Materials Science and Engineering: A, vol. 378, no. 1, pp. 24–33, Jul. 2004. [Online]. Available: https://www.sciencedirect.com/science/article/pii/S0921509303015144

[8] H. Meier, A. Czechowicz, C. Haberland, and S. Langbein, "Smart Control Systems for Smart Materials," Journal of Materials Engineering and Performance,

vol. 20, no. 4, pp. 559–563, Jul. 2011. [Online]. Available: https://doi.org/10.1007/s11665-011-9877-4

[9] G. Scirè Mammano and E. Dragoni, "Effect of Stress, Heating Rate, and Degree of Transformation on the Functional Fatigue of Ni-Ti Shape Memory Wires," Journal of Materials Engineering and Performance, vol. 24, no. 7, pp. 2709–2719, Jul. 2015. [Online]. Available: https://doi.org/10.1007/s11665-015-1561-7

[10] F. Schiedeck and S. Mojrzisch, "Design of a robust control strategy for the heating power of shape memory alloy actuators at full contraction based on electric resistance feedback," Smart Materials and Structures, vol. 20, p. 045002, Mar. 2011.

[11] M. Karhu and T. Lindroos, "Long-term behaviour of binary Ti–49.7Ni (at.%) SMA actuators—the fatigue lives and evolution of strains on thermal cycling," Smart Materials and Structures, vol. 19, no. 11, p. 115019, Sep. 2010. [Online]. Available: https://dx.doi.org/10.1088/0964-1726/19/11/115019

[12] Y. Chemisky, D. J. Hartl, and F. Meraghni, "Three-dimensional constitutive model for structural and functional fatigue of shape memory alloy actuators," International Journal of Fatigue, vol. 112, pp. 263–278, Jul. 2018. [Online]. Available: https://www.sciencedirect.com/science/article/pii/S0142112318301002

[13] C. Calhoun, R. Wheeler, T. Baxevanis, and D. Lagoudas, "Actuation fatigue life prediction of shape memory alloys under the constant-stress loading condition," Scripta Materialia, vol. 95, Jan. 2015.

[14] M. Fumagalli, F. Butera, and A. Coda, "Smartflex NiTi Wires for Shape Memory Actuators," Journal of Materials Engineering and Performance, vol. 18, pp. 691–695, Sep. 2008.

[15] G. S. Mammano and E. Dragoni, "Functional fatigue of shape memory wires under constant-stress and constant-strain loading conditions," Procedia Engineering, vol. 10, pp. 3692–3707, Jan. 2011. [Online]. Available: https://www.sciencedirect.com/science/article/pii/S1877705811007958

[16] V. M. Dornelas, S. A. Oliveira, and M. A. Savi, "A macroscopic description of shape memory alloy functional fatigue," International Journal of Mechanical Sciences, vol. 170, p. 105345, Mar. 2020. [Online]. Available: https://www.sciencedirect.com/science/article/pii/S0020740319330644